

Plasma electrons above Saturn's main rings: CAPS observations

A. J. Coates,¹ H. J. McAndrews,¹ A. M. Rymer,¹ D. T. Young,² F. J. Crary,² S. Maurice,³ R. E. Johnson,⁴ R. A. Baragiola,⁴ R. L. Tokar,⁵ E. C. Sittler,⁶ and G. R. Lewis¹

Received 11 February 2005; revised 21 April 2005; accepted 2 May 2005; published 18 June 2005.

[1] We present observations of thermal ($\sim 0.6\text{--}100\text{eV}$) electrons observed near Saturn's main rings during Cassini's Saturn Orbit Insertion (SOI) on 1 July 2004. We find that the intensity of electrons is broadly anticorrelated with the ring optical depth at the magnetic footprint of the field line joining the spacecraft to the rings. We see enhancements corresponding to the Cassini division and Encke gap. We suggest that some of the electrons are generated by photoemission from ring particle surfaces on the illuminated side of the rings, the far side from the spacecraft. Structure in the energy spectrum over the Cassini division and A-ring may be related to photoelectron emission followed by acceleration, or, more likely, due to photoelectron production in the ring atmosphere or ionosphere. **Citation:** Coates, A. J., et al. (2005), Plasma electrons above Saturn's main rings: CAPS observations, *Geophys. Res. Lett.*, *32*, L14S09, doi:10.1029/2005GL022694.

1. Introduction

[2] It has long been thought that the plasma environment near Saturn's rings would be an interesting one, since it interacts with the dust in the ring system. It had been predicted that the ring 'spokes' seen by Voyager [Smith *et al.*, 1981] might be associated with dynamics affected by dust charging [Goertz and Morfill, 1983; Mendis *et al.*, 1984, and references therein]. In addition, meteoroid impact ionization was predicted to form a thin plasma disk [Ip, 1983] and a neutral particle atmosphere [Ip, 1984], which would likely be an important plasma source for Saturn's inner magnetosphere.

[3] This remarkable environment remained unexplored until the Cassini-Huygens spacecraft flew close to the rings during orbit insertion around Saturn. Initial measurements of the plasma environment [Waite *et al.*, 2005; Young *et al.*, 2005; Tokar *et al.*, 2005] provided a remarkably consistent picture for the gas and plasma composition dominated by O_2^+ and including O^+ . This implies a neutral gas ring atmosphere dominated by O_2

from UV absorption, since any O and H_2O would stick to the cold ring particles, and H_2 would escape [Young *et al.*, 2005; R. E. Johnson *et al.*, Production, ionization and redistribution of Saturn's O2 ring atmosphere, submitted to *Geophysical Research Letters*, 2005]. In addition, data from the Radio and Plasma Wave System (RPWS) provide evidence for meteoroid bombardment in high density regions of the inner Saturn magnetosphere [Gurnett *et al.*, 2004]. The spokes were not observed during SOI, which may be due to viewing geometry or a seasonal effect [Porco *et al.*, 2005].

[4] In this paper we report observations of thermal electrons, which show a remarkable relationship to the physical structure of the rings, and contain information about their formation process.

2. Instrument, Data and Geometry

[5] The Cassini Plasma Spectrometer (CAPS) [Young *et al.*, 2004] is a complementary suite of particle sensors covering ion composition (Ion Mass Spectrometer, IMS), ion beams (Ion Beam Spectrometer, IBS) and electrons (Electron Spectrometer, ELS). The sensors are mounted on an actuator which during this orbit was fixed in positions designed to provide good coverage in the plasma corotation direction. Consequently the pitch angle coverage changes as the spacecraft, and with it the instrument, move with respect to the magnetic field. Here we are concerned with data from ELS [Linder *et al.*, 1998]; an electrostatic analyser with energy range $0.6\text{--}28,000\text{ eV/q}$, $\Delta E/E = 0.17$ and a $160^\circ \times 5^\circ$ field of view split into $8 \times 20^\circ$ sectors, with a best time resolution 2 seconds per energy sweep. If the spacecraft potential is negative, electrons will be retarded in which case ELS measures the high energy tail of the particle distribution. If the spacecraft potential is positive, electrons will be accelerated towards the sensor, which will additionally measure any spacecraft generated photoelectrons with energy lower than the spacecraft potential as well as any naturally occurring low-energy secondary electrons [Johnstone *et al.*, 1997]. Ions on the other hand, will be accelerated by a negative spacecraft potential and retarded by a positive spacecraft potential that will hide any population with energy/charge (E/q) below the spacecraft potential [Tokar *et al.*, 2005].

[6] Cassini's outbound trajectory on the SOI orbit (1 July 2004, DOY 183) was initially above the B, A and F rings. CAPS was switched off for the SOI burn itself for high voltage safety reasons, but operated again from 03:28 UT, while the spacecraft was outbound over the B ring (trajectory line shown on Figure 1 from 03:28 UT, with 10 minute ticks, until 05:00 UT). Cassini was in solar occultation by Saturn between 03:36:51 to

¹Mullard Space Science Laboratory, University College London, Surrey, UK.

²Southwest Research Institute, San Antonio, Texas, USA.

³Observatoire Midi-Pyrénées, Toulouse, France.

⁴Engineering Physics, University of Virginia, Charlottesville, Virginia, USA.

⁵Los Alamos National Laboratory, Los Alamos, New Mexico, USA.

⁶Goddard Space Flight Center, Greenbelt, Maryland, USA.

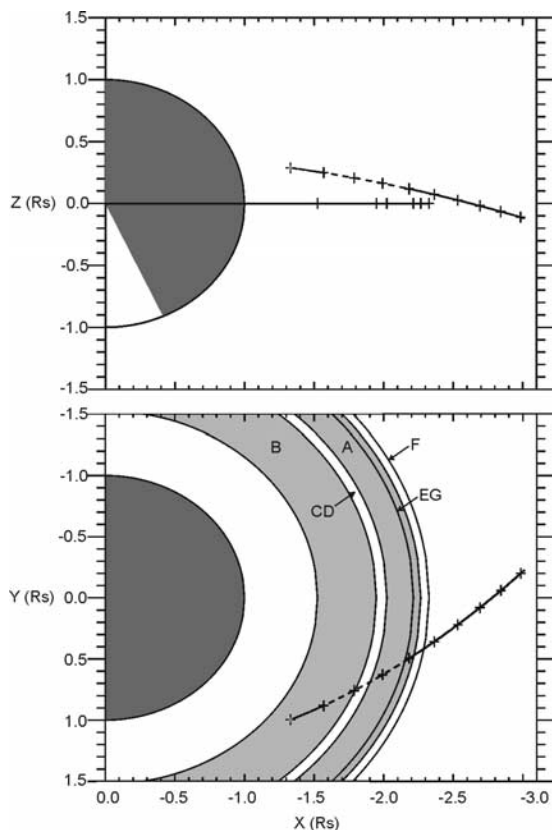


Figure 1. Cassini trajectory and illumination on 1 July 2004. The x-z and x-y planes are shown in a Saturn-centred equatorial coordinate system, in which the Sun is in the x-z plane $\sim 24.5^\circ$ below the x axis. The trajectory line and tick marks start at 03:28 UT, the tick mark spacing is 10 minutes and the trajectory line ends at 05:00 UT. The dashed line indicates when the spacecraft is in Saturn solar occultation. The intersection points (in x-z plot) and concentric circles (x-y plot) outside $1 R_s$ show the B, A and F rings, Cassini Division (CD) and Encke gap (EG).

04:08:40 UT (indicated by the dashed part of the trajectory line in Figure 1).

3. Electron Spectra Over Rings

[7] An electron energy spectrogram is shown in Figure 2. Before and after occultation, the spacecraft photoelectron peak indicates a positive spacecraft potential at this time. During solar occultation the RPWS Langmuir probe (LP) indicates the spacecraft potential is around zero or few volts negative, though there are uncertainties of a few volts in these conditions [Wahlund *et al.*, 2004].

[8] At the end of the plot, penetrating radiation is seen across all ELS energies, due to Saturn's radiation belts. The onset time is precisely when the footprint of a dipole model magnetic field from the spacecraft position to the ring plane leaves the edge of the A ring. During the solar occultation itself, ELS measures the high energy end of the electron spectrum; it may miss a portion of the total electron density while the spacecraft potential is negative, underestimating total density compared to the LP.

[9] The electron population is low intensity when the spacecraft is magnetically conjugate with the B ring (see

Figure 2). When conjugate with the Cassini division, ELS measures a higher electron intensity with structure in energy. When conjugate with the A ring, a medium intensity of electrons is measured, with similar structure in energy. There is also evidence for increased intensity and structure when conjugate with the Encke gap. It should be noted that ELS is sensitive to a range of pitch angles during this period with fairly isotropic distributions somewhat intensified along the field direction (not shown).

[10] Figure 3 shows spectra of the differential energy flux from anode 5, the one least affected by spacecraft-plasma interactions. The spectra are from representative times over (i) the B-ring, (ii) the Cassini division and (iii) the A ring respectively. These plots indicate distinct peaks in spectra (ii) and (iii) at $\sim 3-6$ and ~ 20 eV. These peaks differ somewhat in relative intensity from sample to sample.

[11] In Figure 4, we show the density of electrons within the ELS energy range compared to the optical depth (from Voyager occultation measurements [Esposito *et al.*, 1983], courtesy of PDS rings node (M. Showalter, private communication, 2004)). The density shown here is calculated using a moment integration of phase space density using counts observed in anode 5, assuming 0V spacecraft potential for the interval and assuming isotropy of the measured phase space density. Note that the velocity distribution is that within the energy range of the instrument; so as mentioned above some of the population may be missed if the spacecraft is charged negative. To produce the plot, the ELS data were re-binned as a function of the Cassini magnetic footprint on the ring plane to enable direct comparison with the optical depth results. A large scale, but not precise, anti-correlation appears between the ELS density and the optical depth. However, there is some evidence that the density of these electrons over the Cassini division is enhanced closer to the edge of the B ring.

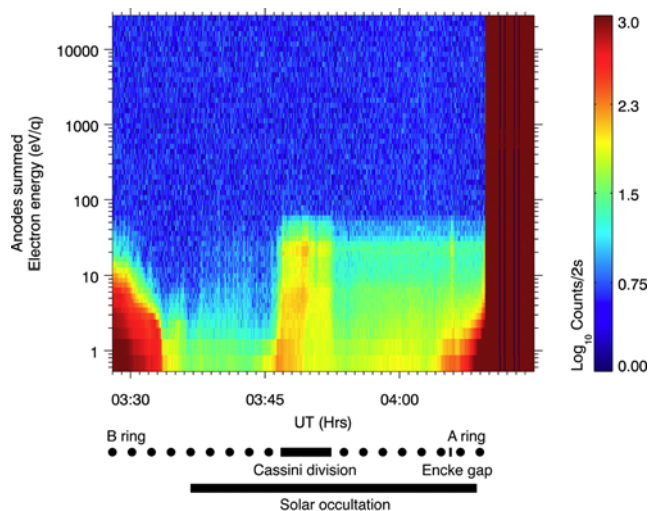


Figure 2. Energy-time spectrogram showing electron counts summed over all anodes. Electron energy is shown on the vertical axis, time on the horizontal axis and the colour scale gives electron counts, proportional to differential energy flux. Solar occultation is shown by the lower solid bar. The times when Cassini is magnetically conjugate with ring features is indicated, using a dipole field model.

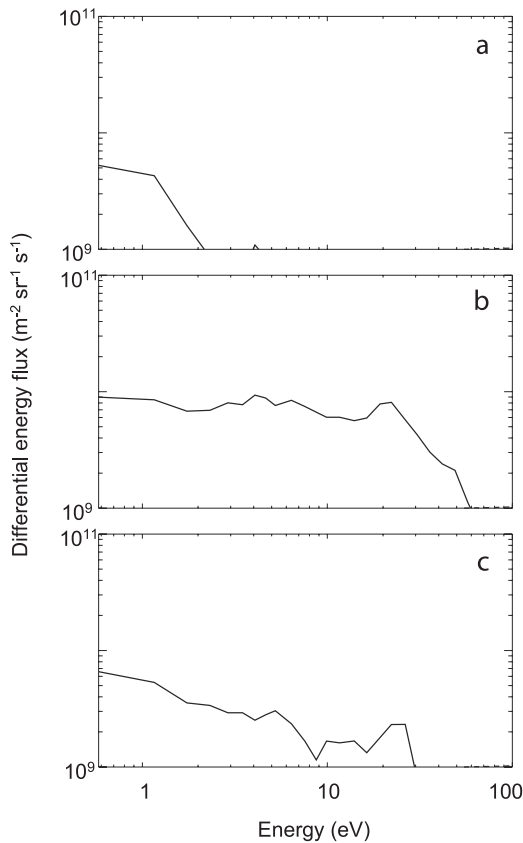


Figure 3. Electron fluxes (32s averages) from anode 5 over (i) B-ring at 03:40 UT, (ii) Cassini division at 03:51 UT, and (iii) A-ring at 03:54 UT.

[12] Figure 5 is a spectrogram covering an extended period with penetrating radiation subtracted. This reveals the low energy (few eV) photoelectron peak, indicating a positive spacecraft potential for the right hand half of the plot. An additional, presumably real, population shows up at ~ 10 eV, with broadly similar character to the spectra over the Cassini division.

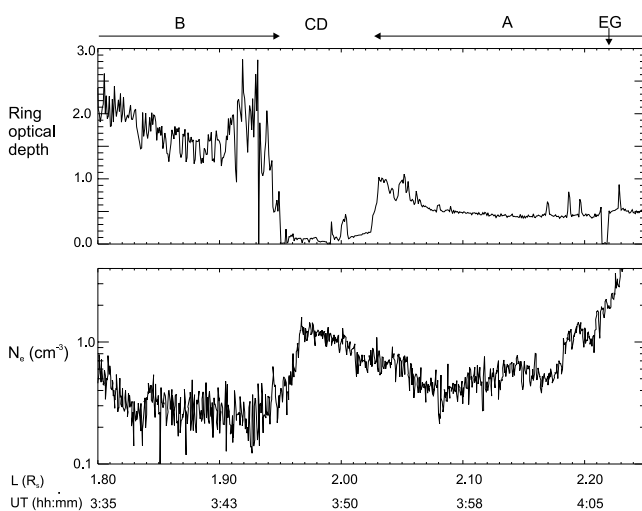


Figure 4. (bottom) Electron density from anode 5 in ELS energy range. (top) Ring optical depth. The B, A, Cassini division (CD) and Encke gap (EG) are indicated.

[13] Figure 1 shows the trajectory geometry in detail. The plot illustrates that the spacecraft may in fact be illuminated through the Cassini division just after the solar occultation period. Immediately after that it is occulted by the A ring, after which full illumination returns when rays beyond the ring edge can reach the spacecraft.

[14] Using this geometric information we can understand the structure in Figure 5 better. After the end of the solar occultation, the spacecraft is initially illuminated through the Cassini division (up to $\sim 04:09:40$ UT, second black ‘sunlit’ bar), producing a positive spacecraft potential φ_{sc} . It is then occulted by the more opaque A ring (at $\sim 04:09:40$ – $04:19:30$), where φ_{sc} is less positive. Following this, full illumination returns at $\sim 04:19:30$ UT and the spacecraft becomes progressively more positive. The latter may be related to the decreasing optical depth of Saturn’s upper atmosphere affecting the intensity of solar illumination reaching the spacecraft as time progresses.

4. Discussion

[15] We observe an increased electron density over the Cassini division, and an approximate anti-correlation of electron density with opacity over the B and A rings. These are consistent with photoelectron emission from the ring particles on the sunlit far side of the rings (i.e., the other, illuminated, side of the ring plane from the spacecraft), as pointed out by *Young et al.* [2005]. This process would yield electrons peaking at a few eV [e.g., *Jurac et al.*, 1995], whereas broad peaks at ~ 3 – 6 and ~ 20 eV are actually observed. If this process were acting alone, then the ~ 3 – 6 eV peak would be associated directly with photoelectrons from the solid ring particles, but an acceleration mechanism would be required to explain the presence of the ~ 20 eV peak. If the ring grains were negatively charged this may provide a possible explanation. Such charging would cause photoelectrons to be accelerated between the photoelectron production point and the spacecraft.

[16] Another process that may produce similar results, and obviate the need for an acceleration mechanism, is UV-produced photoelectrons from the ring atmosphere. The intensity of such photoelectrons, and depending on the

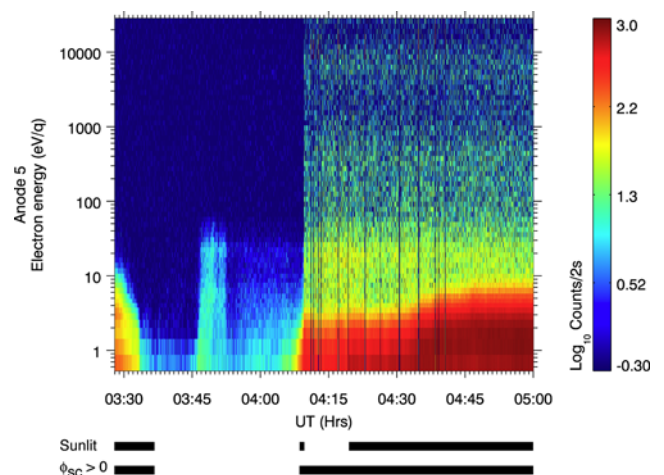


Figure 5. Energy-time spectrogram for anode 5 with penetrating radiation subtracted.

optical depth, the ionisation density, may also reach a peak on the far side of the rings. Again, this would give the observed anti-correlation of electron flux with opacity. One might expect ionospheric photoelectrons with energy ~ 20 eV, similar to those seen at Earth [e.g., Coates *et al.*, 1985], Mars [e.g., Lundin *et al.*, 2004] and Titan (A. J. Coates *et al.*, manuscript in preparation, 2005). After the spacecraft flies over the Cassini division, there may also be a smaller, more local production of photoelectrons in the narrow, sunlit region between the spacecraft and the rings (see Figure 1).

[17] It is interesting to note that calculations of photoionization reactions for O_2 gas give values for the energy of the resulting electrons similar to those we observe at ~ 20 eV. The excess energies are 15.9 and 19.3 eV for solar minimum and maximum photon energies respectively (we expect to be between these two), for $O_2 + h\nu \rightarrow O_2^+ + e$. The excess energies are 23.0 and 27.3 eV for solar minimum and solar maximum for $O_2 + h\nu \rightarrow O + O^+ + e$, 1–2 eV of this would go into nuclear repulsion, with the remainder energy to the photoelectron [Huebner *et al.*, 1992]. The photoelectron energies and timings are consistent with production in the ring exosphere.

[18] Over the Cassini division itself, we note that the density we see is enhanced towards the B ring. This may be a result of increased electron production over the far side of the B ring. In general, the increased electron density that we observe over the Cassini division may be related to the concept of an electron ‘storage ring’ [Ip, 2005], where electrons originating from the plasma near the rings themselves may execute bounce motion relatively unimpeded by ring particles.

[19] There are other potential sources for the electrons. Energetic particles are absent in the CAPS data over the rings, so plasma production from bombardment of the ring (and atmosphere) material is absent from this source. Cosmic ray bombardment has been suggested for production of the ring ionosphere; this would give a positive correlation of density with opacity, whereas the opposite is observed. Meteorite bombardment could provide some of the neutral atmosphere but is unlikely to play a role in ionisation.

[20] In summary, a possible explanation for the peaks at ~ 3 – 6 and ~ 20 eV is direct photoelectron emission from the ring material (~ 3 – 6 eV peak), combined with ionospheric photoelectrons produced in the ring atmosphere/ionosphere (~ 20 eV peak).

5. Summary and Conclusions

[21] The observed electron population seen by ELS over the rings is broadly anti-correlated with ring opacity, has peaks at ~ 3 – 6 and 20 eV over less opaque regions of the rings, and extends beyond the rings themselves in the ring plane.

[22] Our suggested explanation is photoelectron production from ring material producing a broad, low energy (~ 3 – 6 eV) peak, and photoelectron production from the ring atmosphere/ionosphere producing a somewhat narrower, high energy (~ 20 eV) peak.

[23] Further work is needed to quantitatively assess the relative importance of the two sources.

[24] **Acknowledgments.** Work on ELS was supported by PPARC (UK); we thank the entire CAPS team, JPL Cassini project and all the funding agencies which made CAPS a success. Work in the US was performed under JPL contract 1243218 with Southwest Research Institute. We thank T. E. Cravens for a useful discussion on ionospheric photoelectrons. We thank the MSSL CAPS operations team, D. R. Linder, L. K. Gilbert and G. R. Lewis, for support in calibration and data display.

References

- Coates, A. J., A. D. Johnstone, J. F. E. Johnson, J. J. Sojka, and G. L. Wrenn (1985), Ionospheric photoelectrons observed in the magnetosphere at distances of up to 7 Earth radii, *Planet. Space Sci.*, **33**, 1267–1275.
- Esposito, L. W., M. O’Callaghan, R. A. West, C. W. Hord, K. E. Simmons, A. L. Lane, R. B. Pumphrey, D. L. Coffeen, and M. Sato (1985), Voyager PPS stellar occultation of Saturn’s ring, *J. Geophys. Res.*, **88**, 8643–8649.
- Goertz, C. K., and G. Morfill (1983), A model for the formation of spokes in Saturn’s rings, *Icarus*, **53**, 210–220.
- Gurnett, D., W. Kurth, G. Hospodarsky, G. A. Persoon, and A. J. Cuzzi (2004), Evidence of meteoroid impacts on the rings from Cassini plasma wave measurements, *Eos Trans. AGU*, **85**(47), Fall Meet. Suppl., Abstract P51C-06.
- Huebner, W. F., J. J. Keddy, and S. P. Lyon (1992), Solar photorates for planetary atmospheres and for atmospheric pollutants, *Astrophys. Space Sci.*, **195**, 1–294.
- Ip, W.-H. (1983), Equatorial confinement of thermal plasma near the rings of Saturn, *Nature*, **302**, 599–600.
- Ip, W.-H. (1984), Plasmatization and recondensation of the Saturnian rings, *Nature*, **320**, 143–145.
- Ip, W.-H. (2005), An update on the ring exosphere and plasma disc of Saturn, *Geophys. Res. Lett.*, doi:10.1029/2004GL022217, in press.
- Johnstone, A. D., *et al.* (1997), PEACE: A plasma electron and current instrument, *Space Sci. Rev.*, **79**, 351–398.
- Jurac, S., R. A. Baragiola, R. E. Johnson, and E. C. Sittler Jr. (1995), Charging of ice grains by low-energy plasmas: application to Saturn’s E ring, *J. Geophys. Res.*, **100**, 14,821–14,831.
- Linder, D. R., A. J. Coates, R. D. Woodliffe, C. Alsop, A. D. Johnstone, M. Grande, A. Preece, B. Narheim, K. Svensen, and D. T. Young (1998), The Cassini CAPS electron spectrometer, in *Measurement Techniques in Space Plasmas: Particles, Geophys. Monogr. Ser.*, vol. 102, edited by R. E. Pfaff, J. E. Borovsky, and D. T. Young, pp. 257–262, AGU, Washington, D. C.
- Lundin, R., *et al.* (2004), Solar wind induced atmospheric erosion at Mars—First results from ASPERA-3 on Mars Express, *Science*, **305**, 1933–1936.
- Mendis, D. A., J. R. Hill, W.-H. Ip, C. K. Goertz, and E. Grun (1984), Electrodynamic processes in the ring system of Saturn, in *Saturn*, edited by T. Gehrels and M. S. Matthews, Univ. of Ariz. Press, Tucson.
- Porco, C., *et al.* (2005), Cassini Imaging Science: Initial Results on Saturn’s Rings and Small Satellites, *Science*, **307**, 1226–1236.
- Smith, B. A., *et al.* (1981), Encounter with Saturn: Voyager 1 imaging science results, *Science*, **212**, 163–191.
- Tokar, R. L., *et al.* (2005), Cassini observations of the thermal plasma in the vicinity of Saturn’s main rings and the F and G rings, *Geophys. Res. Lett.*, **32**, L14S04, doi:10.1029/2005GL022690.
- Wahlund, J., *et al.* (2004), The ring-dust plasma torus as observed by Cassini RPWS, *Eos Trans. AGU*, **85**(47), Fall Meet. Suppl., Abstract P51A-1406.
- Waite, J. H., Jr. (2005), Oxygen ions observed near Saturn’s A-ring, *Science*, **307**, 1260–1262.
- Young, D. T., *et al.* (2004), Cassini plasma spectrometer investigation, *Space Sci. Rev.*, **114**, 1–112.
- Young, D. T., *et al.* (2005), Composition and dynamics of plasma in Saturn’s magnetosphere, *Science*, **307**, 1262–1265.

R. A. Baragiola and R. E. Johnson, Engineering Physics, University of Virginia, Thornton Hall B103, Charlottesville, VA 22903, USA.

A. J. Coates, G. R. Lewis, H. J. McAndrews, and A. M. Rymer, Mullard Space Science Laboratory, University College London, Surrey RH5 6NT, UK. (ajc@mssl.ucl.ac.uk)

F. J. Crary and D. T. Young, Southwest Research Institute, P. O. Drawer 28510, San Antonio, TX 78228–0510, USA.

S. Maurice, Observatoire Midi-Pyrénées, 9 av. du Colonel Roche, F-31400 Toulouse, France.

E. C. Sittler, Goddard Space Flight Center, Code 910, Greenbelt, MD 20771, USA.

R. L. Tokar, Los Alamos National Laboratory, NIS-1, MS D466, Los Alamos, NM 87545, USA.